

## Electron Density Topological Analysis of Hydrogen Bonding in Glucopyranose and Hydrated Glucopyranose

Roger A. Klein\*

Contribution from the Institute for Physiological Chemistry, University of Bonn,  
53115 Bonn, Germany

Received May 13, 2002

**Abstract:** Topological analysis of the electron density profiles and the atomic basin integration data for the most energetically favorable  ${}^4\text{C}_1$  and  ${}^1\text{C}_4$  conformers of  $\beta$ -D-glucopyranose, calculated at the B3LYP/6-31+G(d), MPWPW91/6-311+G(2d,p), and MP2/6-31+G(d) levels, demonstrates that intramolecular hydrogen bonding between adjacent ring OH groups does not occur in glucopyranose, given the need to demonstrate a bond critical point (BCP) of correct (3,-1) topology for such an interaction to be termed a hydrogen bond. On the other hand, pyranose ring OH groups separated by three, rather than just two, carbon atoms are able to form an intramolecular hydrogen bond similar in topological properties and geometry to that found for propane-1,3-diol. Vicinal, equatorial OH groups in the  ${}^4\text{C}_1$  conformer of glucopyranose are, however, able to form strong bidentate hydrogen bonds with water molecules in a cooperative manner, each water molecule acting simultaneously as both hydrogen bond donor and acceptor, and characterized by (3,-1) bond critical points with increased values for the electron density and the Laplacian of  $\rho(r)$  compared to an isolated ethane-1,2-diol/water complex.

### Introduction

The three-dimensional structures of sugar rings and the way in which their hydroxyl groups are arranged are of biological importance in determining their conformation and the way in which these polyhydric alcohols interact with solvent water, forming the hydration layer, as well as with other molecules. It is generally accepted in the literature that hexopyranoses, as well as other sugars, are able to form intramolecular hydrogen bonds between adjacent, neighboring (vicinal) hydroxyl groups.<sup>1</sup> Ethane-1,2-diol, which can be regarded as a synthon or structural unit for carbohydrate rings, is also considered capable of forming an internal hydrogen bond, albeit weak and relatively strained.<sup>2</sup> The evidence for this view has come mainly from frequency shifts observed in IR and NMR studies,<sup>3</sup> stabilization of the gauche rotamer (as seen using ab initio and MM calculations),<sup>4</sup> together with the use of commonly accepted values for the van

der Waals radii of the hydrogen and oxygen atoms involved.<sup>5</sup> That this view may be erroneous has been indicated in a recent paper concerned with the topological analysis of electron density in a comprehensive series of diols, while highlighting the unfavorable geometry for such an intramolecular hydrogen bond in 1,2-diols<sup>6</sup> ( $d^{\text{O}\cdots\text{H}} \approx 2.3\text{\AA}$  and  $\theta^{\text{O}\cdots\text{H}\cdots\text{O}} \approx 110^\circ$ ). These observations call into serious question the validity of the assumption commonly made in the literature that structures which include ethane-1,2-diol and especially substituted diols, as well as, for example, pyranose and furanose rings, and contain the  $\text{sp}^3\text{-C}$  vicinal diol synthon in the  $\pm$  gauche conformation, are stabilized by an intramolecular hydrogen-bond between neighboring hydroxyl groups rather than by any other form of intramolecular interaction. On the basis of our results, however, intramolecular hydrogen-bonding is possible in ( $n, n + 2$ ) diols such as propane-1,3-diol or in hexopyranose/hexofuranose rings between the 6- $\text{CH}_2\text{OH}$  and 4-OH groups, for example.

### Results and Discussion

Electron densities were calculated from high quality wave function data for the  $\text{g}^+$ - and *trans*-hydroxymethyl conformers of  ${}^4\text{C}_1$  D-glucopyranose, and for the  $\text{g}^+$ -hydroxymethyl conformer of  ${}^1\text{C}_4$  D-glucopyranose. The electron density topology for the lowest energy conformer of the  ${}^4\text{C}_1$  chair form of  $\beta$ -D-glucopyranose, with the hydroxymethyl group  $\text{g}^+$ , is character-

\* To whom correspondence should be addressed. E-mail: klein@institut.physiochem.uni-bonn.de.

- (1) Mendonca, S.; Johnson, G. P.; French, A. D.; Laine, R. A. *J. Phys. Chem. A* **2002**, *106*, 4115–4124; Lewis, B. E.; Schramm, V. L. *J. Am. Chem. Soc.* **2001**, *123*, 1327–1336; Schmidt, R. K.; Karplus, M.; Brady, J. W. *J. Am. Chem. Soc.* **1996**, *118*, 541–546; Liu, Q.; Brady, J. W. *J. Am. Chem. Soc.* **1996**, *118*, 12 276–12 286; Barrows, S. E.; Dulles, F. J.; Cramer, C. J.; French, A. D.; Truhlar, D. G. *Carbohydr. Res.* **1995**, *276*, 219–251; Polavarapu, P. L.; Ewig, C. S. *J. Comput. Chem.* **1992**, *13*, 1255–1261; Ha, S. N.; Madsen, L. J.; Brady, J. W. *Biopolymers* **1988**, *27*, 1927–1952.
- (2) Reiling, S.; Brickmann, J.; Schlenkrich, M.; Bopp, P. A. *J. Comput. Chem.* **1996**, *17*, 133–147; Reiling, S.; Schlenkrich, M.; Brickmann, J. *J. Comput. Chem.* **1996**, *17*, 450–468; Manivet, P.; Masella, M. *Chem. Phys. Lett.* **1998**, *288*, 624–646; Lii, J.-H.; Ma, B.; Allinger, N. L. *J. Comput. Chem.* **1999**, *20*, 1593–1603; Naidoo, K. J.; Kuttel, M. *J. Comput. Chem.* **2001**, *22*, 445456; Momany, F. A.; Willett, J. L. *J. Comput. Chem.* **2000**, *21*, 1204–1219; Crupi, V.; Majolino, D.; Migliardo, P.; Venuti, V. *J. Phys. Chem. A* **2000**, *104*, 11 000–11 012; Bultinck, P.; Van Alsenoy, C.; Goeminne, A. *J. Phys. Chem. A* **2001**, *105*, 9203–9210.
- (3) Crupi, V.; Maisano, G.; Majolino, D.; Migliardo, P.; Venuti, V. *J. Chem. Phys.* **1998**, *109*, 7394–7404; Crupi, V.; Maisano, G.; Majolino, D.; Migliardo, P.; Venuti, V. *J. Phys. Chem. A* **2000**, *104*, 3933–3939.

- (4) Almlöf, J.; Stymne, H. *Chem. Phys. Lett.* **1975**, *33*, 118–120; Bultinck, P.; Goeminne, A.; Van der Vondel, D. *J. Mol. Struct. (THEOCHEM)* **1995**, *334*, 101–107; Bultinck, P.; Goeminne, A.; Van der Vondel, D. *J. Mol. Struct. (THEOCHEM)* **1995**, *357*, 19–32.
- (5) Bondi, A. *J. Phys. Chem.* **1964**, *68*, 44–; Pauling, L. C. *The Nature of the Chemical Bond* 2nd ed., Cornell University Press: Ithaca, New York **1946**, 187–193; Rowland, R. S.; Taylor, R. *J. Phys. Chem.* **1996**, *100*, 7384–7391.
- (6) Klein, R. A. *J. Comp. Chem.* **2002**, *23*, 585–599.

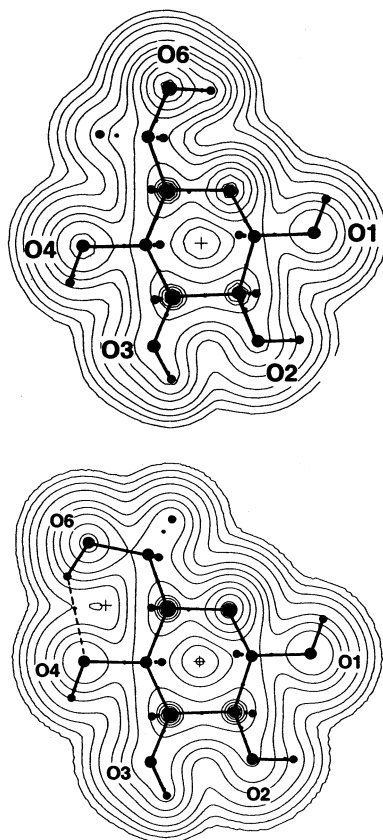


**Figure 1.** (a) Electron density profile for D-glucopyranose  ${}^4C_1$   $g^+$  conformer in the plane of the pyran ring. All bonds other than the C–H bonds are shown: crosses indicate (3,+1) ring critical points (RCPs); cage critical points (CCPs) are shown by a small rectangle; noncovalent (3,–1) bond critical points (BCPs) are shown by small asterisks with covalent (3,–1) BCPs shown with small dots. Contours are drawn at electron densities of 0.001, 0.002, 0.004, 0.008, 0.020, 0.040, 0.080 ..... a.u. Wave functions were obtained using the MPW1PW91/6-311+G(2d,p) hybrid density functional basis-set combination, and were written as 6D 10F Cartesian functions. (b) Electron density profile for D-glucopyranose  ${}^4C_1$  trans conformer in the plane of the pyran ring, showing the O6H···O4 hydrogen bond, with its BCP, resulting from the rotation of the hydroxyl methyl group at C6.

ized by the absence of bond critical points (BCPs) of (3,–1) topology, except for those atoms pairs that are covalently bonded to one another, and by a single ring critical point (RCP) of (3,+1) topology in the center of the pyranose ring (Figure 1 a); there are no BCPs found for the interaction between adjacent ring hydroxyl groups.

A hydrogen bond can be defined as the interaction between an electron-deficient hydrogen atom and an electron-rich region such as an electronegative atom, e.g., O, N, F, or  $\pi$ -electron cloud, together with the presence of two of Popelier's criteria<sup>7</sup> based on Bader's AIM theory,<sup>8</sup> namely a bond critical point (BCP) and an atomic bond path. Hydrogen bonding is highly directional, depending on both donor-acceptor separation and the  $-Y-H\cdots X-$  angle subtended. Modern ideas of hydrogen bonding acknowledge that these interactions can be mainly due to electrostatic and polarization effects, or may consist of a very large covalent component,<sup>9,10</sup> with values for the Laplacian of

**Table 1.** Properties of the Electron Density at the Bond Critical Points for Non-covalent Interactions in Various Glucopyranose Conformers

	$\rho(r)$	$\nabla^2\rho(r)$	energy <sup>a</sup>	Å	$\theta$ (deg)
${}^4C_1$ trans <sup>b</sup>	0.02002	0.08052	–4.63	2.040	135.3
O6–H···O4					
${}^1C_4$ gauche <sup>+b</sup>	0.02181	0.07747	–4.96	2.043	138.3
O1–H···O6					
O2–H···O4	0.02213	0.08420	–5.16	2.010	139.0
O3–H···O1	0.02670	0.09701	–6.54	1.940	142.1
C6–H···O3	0.01160	0.04067	–2.29	2.440	125.4

The H···O geometry is also shown. The wave function used was generated at the MPW1PW91/6-311+G(2d,p) 6D 10F level. <sup>a</sup> estimated interaction energy in kcal/mol, based on the value of the Laplacian of  $\rho$ ,  $\nabla^2\rho(r)$ , and the kinetic energy density,  $G(r)$  – Espinosa et al.<sup>16</sup> <sup>b</sup> defined by the dihedral O5–C5–C6–O6.

$\rho(r)$  at the BCP being either positive (electron depletion) or negative (electron concentration). On the basis of this definition, there are no intramolecular hydrogen bonds between the vicinal OH groups as found in 1,2-diols or hexopyranose rings. Isolated reports had suggested that this might be the case.<sup>11</sup> The  ${}^4C_1$  chair form with the hydroxymethyl group in the trans configuration is, however, capable of forming an intramolecular hydrogen bond characterized by a BCP of (3,–1) topology across the ring between O6H···O4, formally equivalent to a propane-1,3-diol unit (Figure 1b). Of the eight criteria suggested by Popelier, the presence of a (3,–1) BCP and an atomic bond path are crucial; it has been pointed out by Hobza and Havlas that the use of all eight criteria is cumbersome and too reliant on calculation to be of practical use to experimentalists.<sup>12</sup> Despite this criticism Popelier's criteria, based as they are on properties derived from the electron density and atomic basin integration, provide a useful way of determining whether a hydrogen bond in the conventional sense is present in any particular structure, as opposed to a long-distance interaction without overlapping electron distributions.

The  ${}^1C_4$  conformer of glucopyranose, on the other hand, shows three clear intramolecular hydrogen bonds across the ring, i.e., O1H···O6, O2H···O4, and O3H···O1, characterized by BCPs with (3,–1) topology, but again not involving vicinal hydroxyl groups. An additional and unexpected weak interaction is seen for C6H···O3, for which the electron density and Laplacian of  $\rho(r)$  at the bond critical point are both smaller than those of typical hydrogen bonds. Although this observation implies that the two CH<sub>2</sub> hydrogen atoms may be distinguished under certain conditions, conformational averaging over all possible conformers will ensure that the two protons are chemically equivalent unless a particular conformation can be “frozen out”, for example by complexation.

Values of the electron density,  $\rho(r)$ , and the Laplacian of  $\rho(r)$  at the bond critical point, the estimated interaction energy and the geometrical parameters for the various noncovalent interactions in the  ${}^4C_1$  and  ${}^1C_4$  conformers of glucose, are shown in Table 1. Electron density contour maps for the  ${}^1C_4$  conformer through the plane of the ring and orthogonal to the ring are shown in Figure 2a,b. The topology shows a total of six (3,+1) ring critical points (RCPs) and one (3,+3) cage critical point

(7) Koch, U.; Popelier, P. L. A. *J. Phys. Chem.* **1995**, *99*, 9747–9754; Popelier, P. L. A. *J. Phys. Chem. A* **1998**, *102*, 1873–1878.  
 (8) Bader, R. W. F.; “Atoms in Molecules. A Quantum Theory” Clarendon Press: Oxford. *International Monographs on Chemistry* **1990**, *22*, 1–438.  
 (9) Dannenberg, J. J.; Haskamp, L.; Masunov, A. *J. Phys. Chem. A* **1999**, *101*, 7083–7086.

(10) Isaacs, E. D.; Shukla, A.; Platzman, P. M.; Hamann, D. R.; Barbiellini, B.; Tulk, C.A. *Phys. Rev. Lett.* **1999**, *82*, 600–603.  
 (11) Manivet, P.; Masella, M. *Chem. Phys. Lett.* **1998**, *288*, 642–646; Maleknia, S.; Friedman, B. R.; Abedi, N.; Schwartz, M. *Spectroscop. Lett.* **1980**, *13*, 777–784.  
 (12) Hobza, P.; Havlas, Z. *Chem. Rev.* **2000**, *100*, 4253–4264.

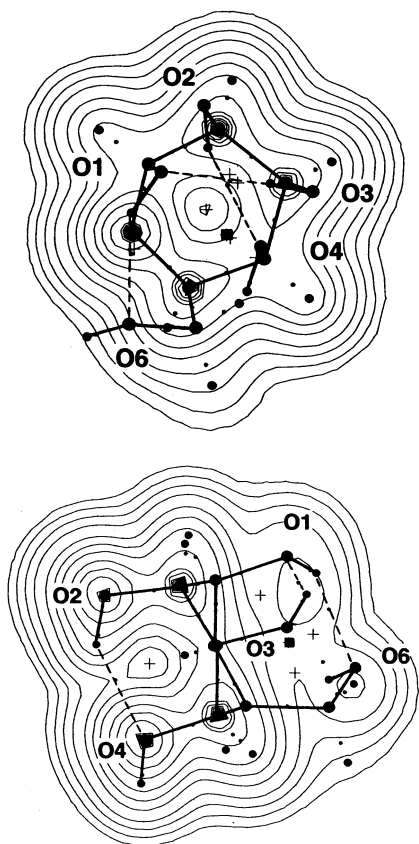


**Figure 2.** (a) Electron density profile for D-glucopyranose  ${}^1C_4 g^+$  conformer in the plane of the pyran ring. (b) Electron density profile for D-glucopyranose  ${}^1C_4 g^+$  conformer in the plane of the O2H $\cdots$ O4 hydrogen bond orthogonal to the plane of the pyran ring.

(CCP), reflecting the across-ring interactions.  $\beta$ -D-glucopyranose- ${}^1C_4 g^+$  (C) also shows an interaction between one of the hydroxymethyl CH<sub>2</sub> protons and O3, manifest by a (3, -1) BCP, as shown in Figure 2b; values for  $\rho(r)$  and  $\nabla^2\rho(r)$  at this BCP are 0.01040 and 0.03754, respectively, giving an interaction energy of -2.5 kcal/mol which is weak compared to the other interactions listed in Table 1 with interaction energies in the range -5.5 to -7.5 kcal/mol.

Atomic basin integration yields values for the atomic charge,  $q(\Omega)$ , and the dipolar polarization,  $\mu(\Omega)$ . These values are shown in Table 2 for all oxygen atoms and hydroxyl hydrogens, together with the Mulliken charges for reference; values for hydroxymethyl CH protons are also shown. Charges derived by AIM theory atomic basin integration have been shown to be among the most accurate and to be preferred over other methods.<sup>13</sup> The calculated Mulliken charges are markedly dependent on the basis-set, (6-31+G(d) gives higher charges than 6-311+G(2d,p)), but less so on the correlation functional used, whereas those derived from atomic basin integration are more stable showing variations in the third or fourth decimal place for the different levels of theory. Atoms involved as hydrogen bond donors or acceptors are shown in bold face in the table.

The OH group hydrogen atoms in  $\beta$ -D-glucopyranose- ${}^4C_1 g^+$  (Table 2, column (A)) are characterized by values for Mulliken charge,  $q^M$ , integrated charge,  $q(\Omega)$ , and dipole polarization,  $\mu(\Omega)$ , of  $0.490 \pm 0.010$ ,  $0.5733 \pm 0.0060$ , and  $0.1668 \pm 0.0029$

au, respectively. These values for  $q(\Omega)$  and  $\mu(\Omega)$  should be compared to those for the “donor” hydrogen atom in 1,2-diols of  $0.5669 \pm 0.0018$  and  $0.1562 \pm 0.0005$  au, and for the nonbonded or free H atom in 1,2-diols of  $0.5537 + 0.0021$  and  $0.1637 + 0.0016$ , respectively.<sup>6</sup> Minor differences would be expected because in 1,2-diols, the interaction -O-H $\cdots$ O-H is single and isolated, whereas in hexopyranoses, it is not, and the sequence can be either clockwise or counterclockwise round the pyran ring.

Both the  $\beta$ -D-glucopyranose- ${}^4C_1$  trans (B) and the  $\beta$ -D-glucopyranose- ${}^1C_4 g^+$  (C) conformers show across-ring hydrogen bonding, evidenced by a (3, -1) BCP, between OH groups in a 1,3-diol configuration, namely, O6H $\cdots$ O4 for (B) and O1H $\cdots$ O6, O2H $\cdots$ O4, and O3H $\cdots$ O1 for (C). In all cases, the donor hydrogen atom shows a small positive increase in atomic charge and a decrease in dipolar polarization, similar to that observed for hydrogen bonding in a range of 1,3-diols<sup>6</sup> with average values for  $q(\Omega)$  and  $\mu(\Omega)$  of  $0.5566 \pm 0.0039$  and  $0.1639 \pm 0.0026$  au (non-interacting H atom) and  $0.5867 \pm 0.0021$  and  $0.1383 \pm 0.0018$  au (interacting or donor H atom), respectively.

In our previous study of diols<sup>6</sup>, it was noted that the oxygen atom attached to the donor hydrogen, H<sub>D</sub>, carried increasing negative charge,  $q(\Omega)$ , and a lower value for the dipolar polarization,  $\mu(\Omega)$ , compared to the acceptor oxygen atom, O<sub>A</sub>, for which the dipolar polarization,  $\mu(\Omega)$ , rose and the atomic volume,  $\text{vol}(\Omega)$ , decreased markedly as the geometry and strength of hydrogen bonding improved. Similar trends are seen in Table 2, especially for the dipolar polarization and atomic volume (data not shown) of the acceptor oxygen atoms involved in hydrogen bonding.

In aqueous solution, there is also no evidence based on MD simulations for a preferred interaction between vicinal OH groups in hexopyranoses, as seen in the gas phase.<sup>14</sup> It seems likely, therefore, based on our results for 1:1 ethane-1,2-diol/water complexes, that the first hydration shell will consist of water molecules intermolecularly hydrogen-bonded in a bidentate manner between the ring hydroxyl groups, acting as both hydrogen bond donors and acceptors in a highly cooperative manner around the pyranose ring.<sup>6,15</sup> In Figure 3A, we show the electron density profile calculated through the plane of the pyran ring of  ${}^4C_1$  glucopyranose hydrated with six water molecules, arranged in such a cooperative, alternating donor-acceptor manner with the ring hydroxyl groups. Figure 3B shows a ball-and-stick representation of this same structure. This structure represents only one of a number of possible, nearly iso-energetic conformations, currently at the practical computational limit for full optimization and frequency calculation at the level of theory used (B3LYP/6-31+G(d,p)) with a fast dedicated work station (~10 days CPU time with 2 GB RAM, dependent on good starting geometry and not being trapped on a very flat potential energy surface (PES), a problem which becomes more severe as the number of hydrogen-bonded water molecules increases).

Table 3 shows the analysis of the BCPs between the six water molecules and the oxygen atoms of the hexopyranose ring in terms of electron density,  $\rho(r)$ , its Laplacian,  $\nabla^2\rho(r)$ , the calculated energy of interaction,  $E^{G(r)}$ , and the bond geometry in Å (-O $\cdots$ H<sub>D</sub>-) and degrees (-O-H<sub>D</sub> $\cdots$ O-). Values for the two most stable 1:1 complexes between ethane-1,2-diol and

(13) Wiberg, K.; Rablen, P. R. *J. Comput. Chem.* **1993**, *14*, 1504–1518.

(14) Molteni, C.; Parrinello, M. *J. Am. Chem. Soc.* **1998**, *120*, 2168–2171.

(15) Brady, J. W.; Schmidt, R. K. *J. Phys. Chem.* **1993**, *97*, 958–966.



**Table 2.** Atomic Properties of the Hydrogen and Oxygen Atoms Involved in the Ring OH Interactions, Showing the Mulliken Charges and the Charge and Dipolar polarization Obtained by Atomic Basin Integration of the Wave Function, Which was Generated at the MPW1PW91/6-311+G(2d,p) 6D 10F Level

atom	glucose ${}^4C_1$ gauche <sup>+</sup> (A)			glucose ${}^4C_1$ trans <sup>+</sup> (B)			glucose ${}^4C_1$ gauche <sup>+</sup> (C)		
	$q^{Ma}$	$q(\Omega)^b$	$\mu(\Omega)^c$	$q^{Ma}$	$q(\Omega)^b$	$\mu(\Omega)^c$	$q^{Ma}$	$q(\Omega)^b$	$\mu(\Omega)^c$
O18	-0.43	-1.1095	0.1741	-0.431	-1.1092	0.1636	-0.571	-1.1342	0.1737
OH1	0.293	0.5704	0.1583	0.295	0.5727	0.1575	0.355	0.6043	0.1356
O2	-0.467	-1.1045	0.1537	-0.466	-1.1037	0.1532	-0.434	-1.1133	0.1799
OH2	0.302	0.5752	0.1548	0.302	0.5759	0.1545	0.320	0.5929	0.1137
O3	-0.463	-1.1032	0.1531	-0.466	-1.1043	0.1528	-0.409	-1.1199	0.1777
OH3	0.301	0.5772	0.1537	0.301	0.5782	0.1533	0.311	0.5966	0.1337
O4	-0.436	-1.0976	0.1601	-0.489	-1.1088	0.1628	-0.469	-1.0934	0.1727
OH4	0.299	0.5765	0.1532	0.308	0.5836	0.1504	0.283	0.5583	0.1647
O5	-0.412	-1.0734	0.0622	-0.361	-1.0640	0.0715	-0.412	-1.0698	0.0681
O6	-0.419	-1.0871	0.1546	-0.430	-1.1075	0.1669	-0.458	-1.0877	0.1599
OH6	0.285	0.5606	0.1601	0.307	0.5877	0.1393	0.287	0.5634	0.1616
C6H	0.152	0.0701	0.1397	0.119	0.0218	0.1594	0.130	0.0261	0.1559
C6H	0.123	0.0262	0.1585	0.127	0.0500	0.1501	0.156	0.0716	0.1314

<sup>a</sup> Mulliken charge in au. <sup>b</sup> Integrated atomic basin charge in au. <sup>c</sup> Dipolar polarization in au.<sup>13</sup>

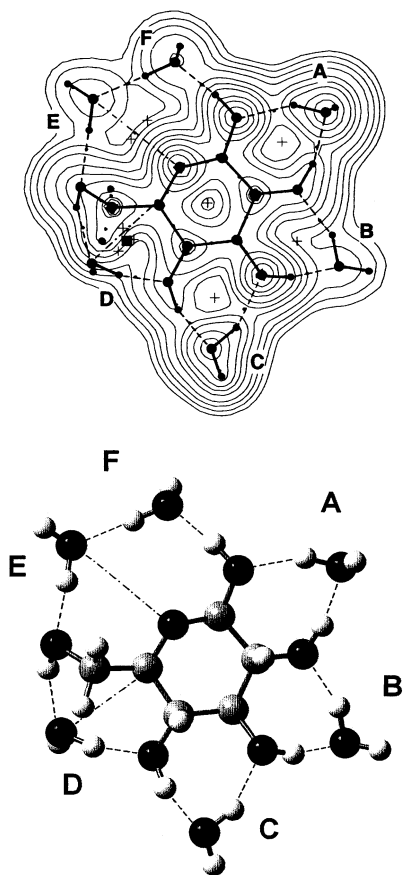


**Figure 3.** (a) Electron density profile for D-glucopyranose  ${}^4C_1$  with six waters of hydration, through the plane of the pyran ring, showing the cooperative bidentate hydrogen bond formation to each water molecule acting simultaneously as donor and acceptor. (b) Ball-and-stick drawing for D-glucopyranose  ${}^4C_1$  with six waters of hydration, corresponding to (a).

water,<sup>6</sup> calculated at this level of theory, are also shown for comparative purposes. At the levels of theory used in this paper, the electron density at the BCP is relatively insensitive to the basis-set used, showing variation in the third or fourth significant figure (approximately  $\pm 1\%$ ), with interaction energies within  $\pm 0.1$  kcal/mol. On the other hand, the Laplacian,  $\nabla^2\rho(r)$ , and the kinetic energy density,  $G(r)$ , show much greater variation ( $\pm 10\text{--}20\%$ ) which nonetheless self-compensate when  $E^{G(r)}$  is calculated. The geometries obtained were within approximately  $\pm 2^\circ$  and  $\pm 0.010$  Å.

**Table 3.** Properties of the Electron Density at the (3,-1) Bond Critical Points for Non-Covalent-H $\cdots$ O-interactions in  ${}^4C_1$ -D-glucopyranose with Six Waters of Hydration

	interaction	$\rho(r)$	$\nabla^2\rho(r)$	energy <sup>a</sup>	Å	$\theta$ (deg)
A	-O-H $\cdots$ OH <sub>2</sub>	0.03624	0.10664	-8.43	1.783	165.0
	H-O-H $\cdots$ O-H	0.03353	0.10300	-8.06	1.814	153.3
B	-O-H $\cdots$ OH <sub>2</sub>	0.03574	0.10449	-8.30	1.793	164.1
	H-O-H $\cdots$ O-H	0.03404	0.10214	-8.14	1.813	153.9
C	-O-H $\cdots$ OH <sub>2</sub>	0.03600	0.10531	-8.41	1.792	160.2
	H-O-H $\cdots$ O-H	0.03421	0.10043	-8.11	1.815	155.5
D	-O-H $\cdots$ OH <sub>2</sub>	0.02542	0.07473	-6.16	1.946	148.2
	H-O-H $\cdots$ O-H	0.02935	0.08680	-6.87	1.865	163.2
E	-O-H $\cdots$ OH <sub>2</sub>	0.03876	0.11550	-8.94	1.746	175.6
	H-O-H $\cdots$ O-H	0.03730	0.10899	-8.58	1.769	178.4
F	-O-H $\cdots$ OH <sub>2</sub>	0.04334	0.12835	-10.22	1.702	171.9
	H-O-H $\cdots$ O-H	0.03876	0.11550	-8.94	1.746	175.6
X	O5 $\cdots$ O <sub>E</sub>	0.00252	0.01115	-0.47	3.627	
	CH5 $\cdots$ O <sub>D</sub>	0.00613	0.02386	-1.18	2.838	
I	-O-H $\cdots$ OH <sub>2</sub>	0.02784	0.08018	-6.56	1.904	160.0
	H-O-H $\cdots$ O-H	0.03042	0.09089	-7.26	1.860	156.1
II	-O-H $\cdots$ OH <sub>2</sub>	0.02792	0.07834	-6.52	1.910	162.3
	H-O-H $\cdots$ O-H	0.03059	0.08817	-7.32	1.874	152.0

The hydrogen bond length and -O-H $\cdots$ O geometry is also shown. The wave function used was generated at the B3LYP/6-31+G(d,p) 6D 10F level (see text). Reference values for the two most stable complexes of ethane-1,2-diol with water, complex (I) *TGg'* and complex (II) *GGg'*,<sup>6</sup> calculated at this level of theory, are also given. <sup>a</sup> estimated interaction energy in kcal/mol, based on the value of the Laplacian of ( $\rho$ ),  $\nabla^2\rho(r)$ , and the kinetic energy density,  $G(r)$  - Espinosa et al.<sup>16</sup> A-F refer to the glycol-water units shown in Figure 3; X refers to additional weak interactions (see discussion in text); I and II refer to the two 1:1 ethane-1,2-diol/water complexes with cooperatively bidentate hydrogen bonded water acting as both donor and acceptor, previously published.<sup>6</sup>

The values of the electron density,  $\rho(r)$ , and the Laplacian of rho,  $\nabla^2\rho(r)$ , at the (3,-1) BCPs for the hydrogen bonds linking the water molecules to the glucopyranose vicinal OH groups are higher than those for bidentate ethane-1,2-diol/water complexes.<sup>6</sup> For example,  $\rho(r)$  at the hydrogen bond critical point for the 1:1 complexes with water acting as either a single donor or acceptor, as a noncooperative bi-acceptor, or as a cooperative donor and acceptor, are 0.027, 0.019, and 0.028–0.030 au, respectively.<sup>6</sup> Multiple cooperativity, as seen in hydrated  ${}^4C_1$  glucopyranose (Figure 3) in which adjacent glycol-water units can interact, results not only in increased electron density at the O-H $\cdots$ O BCPs, some 20–40% higher (0.033–0.043 au) than even in the bidentate glycol-water complexes,<sup>6</sup> as well as its Laplacian,  $\nabla^2\rho(r)$ , but also in the interaction energy based either on the potential energy density  $V(r)$ , derived from the values of the Laplacian and the kinetic energy density  $G(r)$ ,

**Table 4.** Calculated OH Stretching Vibrations in the IR Spectrum of D-glucopyranose  $^4C_1$  with Six Waters of Hydration

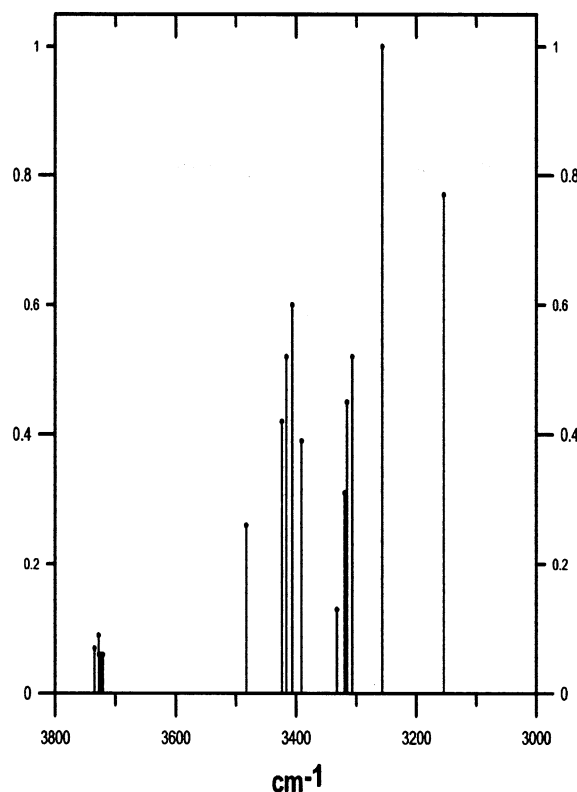
OH stretching absorption $cm^{-1}$	relative intensity 1.0 = 1456.3 km/mole	assignment
3155	0.77	e, f; OH1
3257	1.00	e, f; OH1
3307	0.52	b, c; OH2, OH3, OH4
3316	0.45	e, f; OH1
3319	0.31	a,b,c,d,e,f; OH2,0 H4
3332	0.13	a, b, c, d; OH2, OH3, OH4
3391	0.39	b, c, d; OH4
3407	0.60	a, b, c, d; OH3
3416	0.52	a, d; OH2, OH3, OH4, OH6
3424	0.42	a, b, c, d; OH1, OH2, OH3, OH4, OH6
3483	0.26	d; OH6
3721	0.06	e; $H_{nb}$
3725	0.05	f; $H_{nb}$
3726	0.06	a; $H_{nb}$
3728	0.06	b, c; $H_{nb}$
3728	0.09	b, c; $H_{nb}$
3735	0.07	d; $H_{nb}$

Values were obtained at the B3LYP/6-31+G(d,p) level and have been scaled (scaling factor = 0.9577) as described in the text. Intensities are shown relative to the absorption at  $3257\text{ cm}^{-1}$  (rel int. 1.0 = 1456.3 km/mole). The small letters a–f refer to the water–glycol units A–F indicated in Figure 3a,b;  $H_{nb}$  refers to the non-hydrogen bonded water hydrogen atoms. Vibrations were assigned by inspection using GaussView graphical software.

or NBO analysis of the  $n_O \rightarrow \sigma_{OH}^*$  charge transfer.<sup>16,17</sup> The values for the primary OH6 are more similar to those for ethane-1,2-diol and other 1,2-diol 1:1 complexes with water. In addition to the interactions between water and the glucopyranose OH groups, we have observed two very weak interactions (indicated by X in Table 3), both characterized by the presence of a (3,–1) BCP. One of these, between CH5 and the oxygen atom from H<sub>2</sub>O(D), can be classified as a weak hydrogen bond. The other, between the ring O5 and the oxygen atom of H<sub>2</sub>O(E), can be regarded as a weak van der Waals interaction with an interaction energy comparable to kT.

Cooperativity is also manifest in the IR spectrum of hydrated  $^4C_1$  glucopyranose, calculated at the B3LYP/6-31+G(d,p) level of theory; no imaginary frequencies were observed, indicating that the structure in Figure 3 represents a true minimum and not a transition state (first-order saddle point). In Table 4 we show the values obtained for the O–H stretching frequencies. These values have been scaled. Figure 4 shows the same results in the graphical form of a partial IR spectrum. We determined a scaling factor based on comparison of the experimental O–H stretching frequencies for water in the gas phase<sup>18</sup> with values calculated ab initio for the water monomer at the B3LYP/6-31+G(d,p) level, obtaining an average value of 0.9577(23) for the symmetric and asymmetric modes. This value compares well with 0.9614(34) reported by Scott and Radom, or 0.9527

Rel. Int.

**Figure 4.** Calculated IR spectrum for D-glucopyranose  $^4C_1$  with six waters of hydration showing the OH stretching vibrations. Values were obtained at the B3LYP/6-31+G(d,p) level and have been scaled (scaling factor = 0.9577) as described in the text. The individual points correspond to those in Table 3.

obtained by Baker et al. using direct scaling of the primitive valence force constants, for B3LYP/6-31G(d).<sup>19</sup> Use of such a B3-based hybrid density functional together with a split-valence basis set, has been shown to perform better than Hartree–Fock (HF) or Møller–Plesset (MP2) procedures.<sup>17,20</sup>

In Table 4, the small letters a–f represent the individual water molecules A–F shown in Figure 3. Vibrations were visualized using GaussView.<sup>21</sup> The O–H stretch frequencies fall into two groups: (i) asymmetric modes for the non-hydrogen-bonded water hydrogens in the range  $3735\text{--}3721\text{ cm}^{-1}$ ; and (ii) various modes between  $3483$  and  $3155\text{ cm}^{-1}$  for hydrogen-bonded O–H groups acting together cooperatively indicated by groups of letters, e.g., “b,c,d; OH4” means a synchronized vibration involving units B, C, and D, centered on OH4 of the glucopyranose. The 1:1 complexes between ethane-1,2-diol and water yield similar corrected values for the nonbonded and bonded O–H groups of  $3690 \pm 24\text{ cm}^{-1}$  and  $3455 \pm 25\text{ cm}^{-1}$ , respectively (unpublished data).

The red-shift and intensity for the hydrogen-bonded OH stretching modes is well correlated with the strength of the individual interactions as evidenced by increasing electron density at the BCP. For example, the vibrations at  $3155$  and  $3257\text{ cm}^{-1}$  for units E and F, centered on OH1, are associated

- (16) Espinosa, E.; Molins, E.; LeComte, C. *Chem. Phys. Lett.* **1998**, *285*, 170–173; Espinosa, E.; LeComte, C.; Molins, E. *Chem. Phys. Lett.* **1999**, *300*, 745–748; Espinosa, E.; Souhassou, M.; Lachekar, H.; LeComte, C. *Acta Crystallogr. B* **1999**, *55*, 563–572; Espinosa, E.; Molins, E. *J. Chem. Phys.* **2000**, *113*, 5686–5694; Coppens, P.; Abramov, Y.; Carducci, M.; Korjov, B.; Novozhilova, I.; Alhambra, C.; Pressprich, M. R. *J. Am. Chem. Soc.* **1999**, *121*, 2585–2593.
- (17) Curtiss, L. A.; Pochatko, D. J.; Reed, A. E.; Weinhold, F. *J. Chem. Phys.* **1985**, *82*, 2679–2687; Sekusak, S.; Liedl, K. R.; Sabljic, A. *J. Phys. Chem. A* **1998**, *102*, 1583–1594; Tyrell, J.; Weihstock, R. B.; Weinhold, F. *Int. J. Quantum Chem.* **1981**, *19*, 781–; Reed, A. E.; Curtiss, L. A.; Weinhold, F. *Chem. Rev.* **1988**, *88*, 899–926.
- (18) Lide, D. R., Editor-in-Chief. *Handbook of Chemistry and Physics*, 77th ed.; CRC Press: Boca Raton, 1996–1997.

- (19) Scott, A. P.; Radom, L. *J. Phys. Chem.* **1996**, *100*, 16 502–16 513; Baker, J.; Jarzecki, A. A.; Pulay, P. *J. Phys. Chem. A* **1998**, *102*, 1412–1424.
- (20) Baker, J.; Pulay, P. *J. Comput. Chem.* **1998**, *19*, 1187–1204; Jiang, H.; Appaiddo, D.; Robertson, E.; McNaughton, D. *J. Comput. Chem.* **2002**, *23*, 1220–1225.
- (21) GaussView 2.1 available from Gaussian Inc., Pittsburgh, USA.

with very high values for  $\rho(r) = 0.037\text{--}0.043$  au and the Laplacian  $\nabla^2\rho(r) = 0.11\text{--}0.13$  au, compared to those for the vibration at  $3407\text{ cm}^{-1}$  involving units A, B, C, and D ( $0.025\text{--}0.036$  and  $0.075\text{--}0.105$  au, respectively). As seen in Table 3, considerable cooperativity or synchronization between the OH stretching vibrations for adjacent water–glycol units is observed. The O–H stretching vibrations for the hydrogen-bonded O–H groups are, in general, considerably more red-shifted than those for ethane-1,2-diol/water complexes, in which the glycol unit is isolated, i.e., not able to interact cooperatively with its neighbors.

Natural bond orbital (NBO) analysis,<sup>22</sup> using second-order perturbation and Fock matrix-element deletion with the caveat that the interactions are not strongly coupled with other interactions,<sup>17</sup> showed that the interaction energy for the acceptor oxygen LP electrons and the O–H<sub>D</sub>  $\sigma^*$  antibonding orbital in *gauche* ethane-1,2-diol, both as an isolated molecule as well as embedded in <sup>4</sup>C<sub>1</sub>-glucopyranose was approximately 0.4–0.5 kcal/mol, some 10–15 times smaller than for the  $n_{\text{O}} \rightarrow \sigma^*_{\text{OH}}$  interaction in the water dimer. A referee has pointed out that if one uses the modified molecular mechanics MM4 force-field and adds up the van der Waals repulsion and attraction, dipole–dipole and induced dipole interactions for ethylene glycol, the total interaction energy is short by about 0.9 kcal/mol; this is associated with a red-shift of  $32\text{ cm}^{-1}$  and bond shortening of  $0.004\text{ \AA}$ .<sup>23</sup> This suggests that for the MM4 model the “hydrogen bond” in ethylene glycol has a strength of  $\sim\text{--}0.9$  kcal/mol. Using methods mentioned in this paper, we have obtained comparable figures for ethane-1,2-diol and other 1,2-diols, namely  $\text{--}0.4$  to  $\text{--}0.5$  kcal/mol,  $\sim 40\text{ cm}^{-1}$  and  $0.004\text{ \AA}$  (unpublished observations). Interaction energies for the oxygen lone pair electrons and the O–H<sub>D</sub> antibonding orbitals in ethane-1,2-diol 1:1, whether alone or as part of hydrated glucopyranose, forming 1:1 complexes with water in a cooperative, donor–acceptor manner, were comparable with or slightly higher than for the water dimer ( $\sim\text{--}10$  kcal/mol against  $\sim\text{--}7$  kcal/mol).

Changes in occupancy for the  $\sigma^*_{\text{OH}}$  antibonding orbitals reflected the  $n_{\text{O}} \rightarrow \sigma^*_{\text{OH}}$  interaction energies, with the ethane-1,2-diol unit showing values some 15–25% (often barely doubling the non-interacting reference value obtained with the all-trans diol) of those for either the water dimer or the cooperative 1:1 water–diol complexes, irrespective of whether it was an isolated molecule or part of glucopyranose. In 1,2-diols, the  $\text{--O--H}\cdots\text{O--H}$  interaction changes the occupancy of the  $\sigma^*$  antibonding orbital by approximately 0.0020 au. Similar values are observed for the vicinal OH interactions in <sup>4</sup>C<sub>1</sub> glucopyranose (Figure 1). The cross-ring, propane-1,3-diol type interactions seen in <sup>1</sup>C<sub>4</sub> glucopyranose (Figure 2) are

characterized by changes in  $\sigma^*$  occupancy of  $\sim 0.015$  au, similar to that observed for propane-1,3-diol and butane-1,3-diol (unpublished data). Changes in  $\sigma^*$  occupancy for the ring OH groups of cooperatively hydrated <sup>4</sup>C<sub>1</sub> glucopyranose (Figure 3) show values ( $\sim 0.035$  au) in excess of those for 1:1 ethane-1,2-diol/water complexes ( $\sim 0.022$  au). The overall similarity between our present NBO results obtained for ethane-1,2-diol alone or embedded within glucopyranose, including those for the 1:1 complexes with water, further supports the use of this simple 1,2-diol to model computationally the behavior of the hexopyranose ring hydroxyl groups.<sup>6</sup>

## Conclusions

Thus, in conclusion, there is no electron density topological evidence, based on high-level ab initio calculations of the wave functions, to support the view that vicinal hydroxyl groups are capable of forming intramolecular hydrogen bonds in hexopyranose rings. Any intramolecular hydrogen bonds are formed between OH groups ( $n, n + 2$ ) to one another, i.e., at a spacing formally equivalent to that in propane-1,3-diol. Hydrogen bonding between ring OH groups spaced in this way has been reported for  $\beta$ -D-fructofuranose in DMSO solution based on NMR evidence.<sup>24</sup> Although 1,2-diols do show a through-space interaction between the two hydroxyl groups, with stabilization of the *gauche* conformer in preference to the *trans* conformer, this interaction cannot be considered a hydrogen bond in the light of the definition above. Ab initio calculations show that both the IR red-shift and the NMR downfield shift are small compared to established hydrogen bonding interactions, as is the interaction energy (unpublished data). The interaction seen in 1,2-diols is probably a mixture of weak polarization and electrostatic effects.

The model used for what is meant by a hydrogen bond is not just one of semantics. Various approaches to this question are equally valid. Hydrogen bonding may be defined experimentally, i.e., through the observation of spectroscopic shifts, for example, a downfield NMR shift (equivalent to de-shielding) for the proton, or a red-shift to lower wavenumber for the OH stretching vibration. There are problems with using spectroscopic shifts to determine whether a hydrogen bond is present, however, because there exists a continuum of shifts representing very weak through to very strong hydrogen bonds, typically from around  $10\text{ cm}^{-1}$  to more than  $1000\text{ cm}^{-1}$  in the IR or less than 1 ppm to 10 ppm or more for proton NMR, with no quantitative measure of when a very small shift should or should not be considered to be due to hydrogen bonding. Moreover, hydrogen bonds exhibiting a blue shift to higher wavenumber are known, challenging one of the standard experimental methods for detecting hydrogen bonds.<sup>12,25</sup>

Views of what constitutes a hydrogen bond range from purely electrostatic, or electrostatic plus polarization effects, the inclusion of a charge-transfer term, through to possession of considerable covalent character.<sup>9</sup> Strong hydrogen bonds, as found in ice, are substantially covalent; the Compton-scattering angular momentum anisotropy results reported by Isaacs et al.<sup>10</sup> cannot be explained satisfactorily using a purely electrostatic model.

Classical Kitaura–Morokuma energy decomposition analysis, or its variants, breakdown the interaction into electrostatic, polarization, exchange repulsion, and charge-transfer compo-

- (22) Glendenning, E. D.; Badenkoop, J. K.; Reed, A. E.; Carpenter, J. E.; Bohmann, J. A.; Morales, C. M.; Weinhold, F.; NBO 5.0 2001, Theoretical Chemistry Institute, University of Wisconsin, Madison WI, USA.; Glendenning, E. D.; Badenkoop, J. K.; Reed, A. E.; Carpenter, J. E.; Weinhold, F.; NBO 4.0M 1999, Theoretical Chemistry Institute, University of Wisconsin, Madison WI, USA — used in conjunction with PC-GAMESS 6.2 (build 2068) from Granovsky, A. A.; Kress, J.; Burger, P.; Ponec, R.; 2001, Laboratory of Chemical Cybernetics, Moscow State University, Moscow, Russia; Schmidt, M. W.; Baldrige, K. K.; Boatz, J. A.; Elbert, S. T.; Gordon, M. S.; Jensen, J. H.; Koseki, S.; Matsunaga, N.; Nguyen, K. A.; Su, S. J.; Windus, T. L.; together with Dupuis, M.; Montgomery, J. A.; *J. Comput. Chem.* **1993**, *14*, 1347–1363.
- (23) Lii, J.-H.; Allinger, N. L. *J. Comput. Chem.* **1998**, *19*, 1001–1016; Lii, J.-H.; Hydrogen Bonding: 2. In *Encyclopedia of Computational Chemistry*; Schleyer, P. v. R., Allinger, N. L., Clark, T., Gasteiger, J., Kollman, R. A., Schaefer, H. F., III, Schreiner, P. R., Eds.; John Wiley & Sons: Chichester, IUK, 1998; 1271; Lii, J.-H.; Allinger, N. L.; ethylene glycol—unpublished work.

(24) Dais, P.; Perlin, A. S. *Carbohydr. Res.* **1987**, *169*, 159–169.

(25) Liu, L.; Schlegel, H. B. *J. Am. Chem. Soc.* **2002**, *124*, 9639–9647.



nents.<sup>26</sup> Studies of the water dimer, including with a dispersion component, indicate that a major component is the electrostatic interaction.<sup>27</sup> Morokuma decomposition of the monomer–monomer interaction for the water dimer, minimized at the MP2/6-311++G(2d,p) level, yields a total energy of  $-4.40$  kcal/mol, composed of electrostatic, exchange repulsion, polarization, and charge-transfer terms, respectively, of  $-9.25$  kcal/mol,  $+6.94$  kcal/mol,  $-1.25$  kcal/mol, and  $-1.57$  kcal/mol (own unpublished observations using GAMESS software); these values compare well with the extensive data reported by Chen and Gordon for the water dimer at levels of theory up to MP2-(FC)/cc-aug-pVDZ,<sup>28</sup> with a best estimate for the hydrogen-bond energy of  $-5.0 \pm 0.1$  kcal/mol.<sup>29</sup> Using natural bond orbital (NBO) analysis, Weinhold and co-workers have shown that the charge-transfer component predominates, with electrostatic attraction being offset to a large extent by exchange repulsion.<sup>30</sup> Resonance stabilization or cooperativity may enhance the hydrogen bonding interaction, producing shorter donor–acceptor distances, particularly if acting in a concerted or alternating fashion.<sup>6,9</sup> It should be noted in this context that the interaction energies derived from  $\nabla^2\rho(r)$  and  $G(r)$  and given in Tables 1 and 3, or by NBO second-order perturbation analysis, should be compared to the electrostatic component obtained by energy decomposition analysis rather than regarded as total interaction energies.

Detection of a bond critical point (BCP) of (3,−1) topology between a hydrogen-bond donor and acceptor at their equilibrium geometry, implies that the two nuclei are linked by an atomic bond path and share an interatomic surface with electronic charge density accumulation at the BCP, as defined by Bader.<sup>8</sup> The presence of a BCP indicates that there is orbital interaction with overlapping electron distributions. In terms of classifying interactions as hydrogen-bonds, the presence or absence of a (3,−1) BCP has one great advantage. It is either there, or it is not. Thus, there is no need to construct an artificial cutoff point, below which the interaction is not considered to be a hydrogen-bond and above which it is. As pointed out by Bader,<sup>31</sup> "... the presence of a (3,−1) CP and its associated atomic interaction line in such a stable state of electrostatic equilibrium is thus both necessary and sufficient for the two atoms to be bonded to one another in the usual chemical sense of the word..."

Many molecular mechanics force-fields, with the notable exception of MM4, still use a predominantly electrostatic model for the hydrogen bond without adequate parametrization for lone-pair directionality. Molecular mechanics (MM) force-fields generally seem to indicate intramolecular hydrogen-bonding for vicinal diols. It should be remembered, however, that this may be an artifact of the procedures used to parametrize the force-field in question because ethane-1,2-diol is often included in the "training" set.<sup>32</sup> If parametrization is carried out with a

molecule set which includes ethane-1,2-diol, especially if intramolecular hydrogen-bonding is explicitly included, then it is not surprising if the same force-field subsequently provides "evidence" pointing to the presence of hydrogen bonds in similar structures. We have recently pointed out that different MM force-fields behave rather variably in accurately representing long-range, noncovalent interactions such as hydrogen bonds, necessary for predicting physical properties.<sup>33</sup> The ability to accurately model local cluster formation and hydrogen bond cooperativity in the liquid state is likely to be the key to understanding the thermodynamic behavior of water in aqueous solutions.<sup>34</sup>

## Methods

Starting geometries were based on the torsional angles reported by Barrows et al.<sup>35</sup> for structures optimized at the MP2/cc-pVDZ level. Wave function files in Cartesian coordinates (6D 10F) were generated after optimization using the Gaussian98<sup>36</sup> hybrid density functionals B3LYP<sup>37</sup> and MPW1PW91<sup>38</sup> together with the 6-31+G(d) and 6-311+G-(2d,p) basis sets, respectively, as well as at the MP2/6-31+G(d) level, before being analyzed for electron density distribution and topology using both Popelier's Morphy98<sup>39</sup> and Biegler–König's AIM2000.<sup>40</sup> The Gaussian option (scf-tight) was used, as recommended by Popelier, to prevent any "lost charge" during integration. Calculations were also checked at the MP2/6-31+G(d) level since it is known that density functional theory methods do not account correctly for dispersive forces.<sup>41</sup>

**Acknowledgment.** I should like to acknowledge financial support for the work reported here in the form of a project grant as part of a Deutsche Forschungsgemeinschaft Sonderforschungsbereich program grant (Grant No. DFG SFB284/A1). I should also like to thank Ernst Bause and Jacopo Tomasi for helpful discussions.

JA0206947

- (26) Kitaura, K.; Morokuma, K. *Int. J. Quantum Chem.* **1976**, *10*, 325–340; Morokuma, K.; Kitaura, K. *Molecular Interactions*; Ratajczak, H., Orville-Thomas, W. J., Eds.; Wiley: New York, 1980; Vol. 1, pp 21–87; Morokuma, K.; Kitaura, K. *Chemical Applications of Atomic and Molecular Electrostatic Potentials*; Politzer, P., Truhlar, D. G., Eds.; Plenum Press: New York, 1981; pp 215–242.
- (27) Singh, U. C.; Kollman, P. A. *J. Chem. Phys.* **1985**, *83*, 4033–4040; Mo, Y.; Gao, J.; Peyerimhoff, S. D. *J. Chem. Phys.* **2000**, *112*, 5530–5538.
- (28) Chen, W.; Gordon, M. S. *J. Phys. Chem.* **1996**, *100*, 14 316–14 328.
- (29) Liedl, K. R.; Kroemer, R. T. *J. Phys. Chem. A* **1998**, *102*, 1832–1836; Feyereisen, M. W.; Feller, D.; Dixon, D. A. *J. Phys. Chem.* **1996**, *100*, 2993–2997; Xantheas, S. S. *J. Chem. Phys.* **1996**, *104*, 8821–8824.
- (30) Reed, A. E.; Curtiss, L. A.; Weinhold, F. *Chem. Rev.* **1988**, *88*, 899–926.
- (31) Bader, R. F. W. *J. Phys. Chem. A* **1998**, *102*, 7314–7323.
- (32) Momany, F.; Rone, R. *J. Comput. Chem.* **1992**, *13*, 888–900; Reiling, S.; Schlenkrich, M.; Brickmann, J. *J. Comput. Chem.* **1996**, *17*, 450–468.
- (33) Jónsdóttir, S. O.; Welsh, W. J.; Rasmussen, K.; Klein, R. A. *New J. Chem.* **1999**, 153–163.
- (34) Truskett, T. M.; Dill, K. A. *J. Chem. Phys.* **2002**, *117*, 5101–5104.
- (35) Barrows, S. E.; Dulles, F. J.; Cramer, C. J.; French, A. D.; Truhlar, D. G. *Carbohydr. Res.* **1995**, *276*, 219–251; the two most probable conformers for glucopyranose <sup>13</sup>C<sub>1</sub> (with the hydroxymethyl *g*<sup>+</sup> and *trans*) and the most probable one for glucopyranose <sup>13</sup>C<sub>4</sub> *g*<sup>+</sup>, were used.
- (36) Frisch, M. J.; Trucks, G. W.; Schlegel, H. B.; Scuseria, G. E.; Robb, M. A.; Cheeseman, J. R.; Zakrzewski, V. G.; Montgomery, J. A., Jr.; Stratmann, R. E.; Burant, J. C.; Dapprich, S.; Millam, J. M.; Daniels, A. D.; Kudin, K. N.; Strain, M. C.; Farkas, O.; Tomasi, J.; Barone, V.; Cossi, M.; Cammi, R.; Mennucci, B.; Pomelli, C.; Adamo, C.; Clifford, S.; Ochterski, J.; Petersson, G. A.; Ayala, P. Y.; Cui, Q.; Morokuma, K.; Malick, D. K.; Rabuck, A. D.; Raghavachari, K.; Foresman, J. B.; Cioslowski, J.; Ortiz, J. V.; Baboul, A. G.; Stefanov, B. B.; Liu, G.; Liashenko, A.; Piskorz, P.; Komaromi, I.; Gomperts, R.; Martin, R. L.; Fox, D. J.; Keith, T.; Al-Laham, M. A.; Peng, C. Y.; Nanayakkara, A.; Gonzalez, C.; Challacombe, M.; Gill, P. M. W.; Johnson, B.; Chen, W.; Wong, M. W.; Andres, J. L.; Gonzalez, C.; Head-Gordon, M.; Replogle, E. S.; Pople, J. A. *Gaussian 98*, Revision A.7, Gaussian, Inc., Pittsburgh, PA, 1998.
- (37) Lee, C.; Yang, W.; Parr, R. G. *Phys. Rev. B* **1988**, *37*, 785; Miehlich, B.; Savin, A.; Stoll, H.; Preuss, H. *Chem. Phys. Lett.* **1989**, *157*, 200; Becke, A. D. *J. Chem. Phys.* **1993**, *98*, 5648; Pople, J. A.; Head-Gordon, M.; Fox, D. J.; Raghavachari, K.; Curtiss, L. A. *J. Chem. Phys.* **1989**, *90*, 5622; Curtiss, L. A.; Jones, C.; Trucks, G. W.; Raghavachari, K.; Pople, J. A. *J. Chem. Phys.* **1990**, *93*, 2537.
- (38) Becke, A. D. *J. Chem. Phys.* **1996**, *104*, 1040; Adamo, C.; Barone, V. *Chem. Phys. Lett.* **1997**, *274*, 242; Adamo, C.; Barone, V. *J. Comput. Chem.* **1998**, *19*, 418; Adamo, C.; Barone, V. *J. Chem. Phys.* **1998**, *108*, 664.
- (39) MORPHY98, a topological analysis program written by P. L. A. Popelier with a contribution from R. G. A. Bone (UMIST, Engl, EU); Popelier, P. L. A. *Comput. Phys. Comm.* **1996**, *93*, 212–240; Popelier, P. L. A. *Theor. Chim. Acta* **1994**, *87*, 465–476; Popelier, P. L. A. *Mol. Phys.* **1996**, *87*, 1169–1187; Popelier, P. L. A. *Comput. Phys. Comm.* **1998**, *108*, 180–190; Popelier, P. L. A. *Can. J. Chem.* **1996**, *74*, 829–838.
- (40) Biegler-König, F.; Bayles, D.; Schönbohm, J.; 1998–2000.
- (41) Chalasiński, G.; Szczesniak, M. M. *Chem. Rev.* **2000**, *100*, 4227–4252; Tian, S. X.; Chi, X. X.; Xu, K. Z. *Chem. Phys.* **2002**, *276*, 263–276; Valdes, H.; Sordo, J. A. *J. Comput. Chem.* **2002**, *23*, 444–455.